doi:10.14311/ppt.2025.2.164
Plasma Physics and Technology **12**(2):164–169, 2025

MULTI-TEMPERATURE THERMOPHYSICAL PROPERTIES AND QUENCHING CHARACTERISTICS OF ARC PLASMAS IN SF_6 AND ITS ALTERNATIVE

G. Wang, B. Zhang, J. Deng, M. Cao, X. Li*

State Key Laboratory of Electrical Insulation and Power Equipment, Xi'an Jiaotong University, Xi'an, Shaanxi Province, People's Republic of China

* xwli@mail.xjtu.edu.cn

Abstract. Gaseous switching arc plasmas near current zero typically deviate from LTE and are often modeled using a two-temperature approach. However, in non-equilibrium plasmas, different energy states may follow separate Boltzmann distributions, each with distinct temperatures. This study calculates the thermophysical properties of SF_6 and C_4F_7N arc plasmas by explicitly considering translational, rotational, vibrational, and electronic excitation temperatures. The results reveal that compared to the conventional two-temperature model (distinguishing heavy species and electrons), the multi-temperature framework leads to measurable changes in plasma properties. The C_4F_7N mixture is more sensitive to multi-temperature effects than SF_6. Additionally, the two-temperature simulation model may slightly underestimate the plasma's non-equilibrium degree.

Keywords: SF_6, C_4F_7N, arc, non-equilibrium plasma, thermophysical properties, MHD.

1. Introduction

In most previous studies, due to the extremely high temperatures (15∼30 kK) of gas switching arcs, the plasma is generally assumed to satisfy the local thermodynamic equilibrium (LTE) condition. This assumption implies that collisions and energy exchange among different species are sufficiently frequent, and all particles in the plasma are presumed to share the same temperature, which is reasonable for the arc burning phase. Based on the LTE assumption, Murphy et al. [1] and Narayanan et al. [2] have calculated the chemical composition and thermophysical properties of various arc plasmas, providing essential parameters for the numerical simulation of gas arcs. However, in the arc fringes and current-zero regions, where the plasma temperature is relatively low, insufficient energy exchange occurs between electrons and heavy particles due to their significant mass disparity. Consequently, the plasma often exhibits a non-local thermodynamic equilibrium (NLTE) state, where the electron temperature exceeds that of heavy particles. Research has shown that neglecting NLTE effects may lead to erroneous estimations of electron states in the plasma, thereby causing inaccuracies in predicting the breakdown process of switching devices. In this regard, Gleizes et al. [3], and Colombo et al. [4] have investigated the thermophysical parameters of various non-equilibrium plasmas, consistently finding that NLTE conditions significantly influence the thermodynamic and transport properties of gas arcs. In numerical simulations, Wang et al. [5] studied the evolution of NLTE arcs in SF_6 circuit breakers and observed strong non-equilibrium behavior at the arc edges under gas-blast conditions. Furthermore, for plasmas where quantum energy levels follow a Boltzmann distribution, translational, rotational, vibrational, and excitation states may exhibit distinct distributions, each corresponding to different temperature definitions. To further elucidate the influence of NLTE conditions on plasma evolution, it is necessary to investigate the thermophysical properties and interruption characteristics of multi-temperature arcs. Additionally, given the severe greenhouse effect of SF_6 (with a global warming potential approximately 24,300 times that of CO_2), environmentally friendly alternatives for arc quenching media have become a research priority. Among them, C_4F_7N has attracted considerable attention due to its excellent dielectric properties, and C_4F_7N-based gas mixtures have been preliminarily applied in switching devices [6]. However, reliable interruption near current zero remains a significant challenge for C_4F_7N alternatives. According to experimental results from Franck et al. [7], the thermal interruption capability of C_4F_7N–CO_2 mixtures is only about two-thirds that of SF_6. Based on our previous research, the physical properties of eco-friendly gas arcs near current zero may be more significantly affected by NLTE conditions [8]. In summary, this work further investigates the thermodynamic and transport properties of SF_6 and C_4F_7N–CO_2 plasmas under multi-temperature conditions, conducts non-equilibrium magnetohydrodynamic (MHD) simulations for both gas arcs, and compares their NLTE characteristics. The results provide essential data for numerical modeling of NLTE arcs and contribute to a deeper understanding of arc interruption behavior near current zero.

2. Method

This study employs a multi-temperature plasma model to describe the energy states of plasma under non-equilibrium conditions, based on the assumption of local chemical equilibrium (LCE). Due to varying energy exchange rates among different degrees of freedom, the translational, rotational, and vibrational energy levels of particles may follow distinct Boltzmann distributions, each corresponding to a separate temperature definition. For heavy particles, translational kinetic energy rapidly equilibrates on a picosecond timescale through interparticle collisions, allowing the translational temperature (T_{tr}) to be directly defined as the heavy-particle temperature (T_{h}). Similarly, due to the small energy spacing between rotational levels, rotational equilibrium is quickly achieved, making the rotational temperature (T_{rot}) nearly identical to T_{tr} and thus also approximating T_{h}. In contrast, molecular vibrational energy levels exhibit larger spacing, requiring longer relaxation times to reach equilibrium. Consequently, during the cooling phase of arc plasma, the vibrational temperature (T_{vib}) typically exceeds T_{rot}. Furthermore, electronic excitation states possess the largest energy spacing, resulting in an excitation temperature (T_{ex}) that is generally higher and closer to the electron temperature (T_{e}). Previous studies have demonstrated that in non-equilibrium plasmas, the vibrational temperature typically lies between the rotational and excitation temperatures [9]. Following the recommendation of André et al. [10], this study approximates the vibrational temperature as $\sqrt{\theta}$ times the rotational temperature, where θ denotes the degree of non-equilibrium (θ=$T_{\mathrm{e}}/T_{\mathrm{h}}$). In summary, the temperature definitions for multi-temperature plasma in this work are as follows:

$$l\begin{cases} T_{\mathrm{tr(e)}} = T_{\mathrm{e}}; T_{\mathrm{tr(h)}} = T_{\mathrm{h}} \\ T_{\mathrm{rot}} = T_{\mathrm{h}} \\ T_{\mathrm{vib}} = \sqrt{\theta} T_{\mathrm{h}} \\ T_{\mathrm{ex}} = T_{\mathrm{e}} = \theta T_{\mathrm{h}} \end{cases} \tag{1}$$

The determination of plasma composition is a prerequisite for calculating its thermodynamic properties and transport coefficients. For plasmas under the assumption of chemical equilibrium, this study employs the van de Sanden formulation of the mass action law to compute species composition under non-local thermodynamic equilibrium conditions:

$$\frac{n_a n_b}{n_{ab}} = \frac{Z_a Z_b}{Z_{ab}} \left(\frac{2\pi m_a m_b k_{\mathrm{B}} T_{\mathrm{h}}}{m_{ab} h^2} \right)^{3/2} \exp\left(-\frac{E_{\mathrm{d}}}{k_{\mathrm{B}} T_{\mathrm{h}}} \right) \tag{2}$$

$$\frac{n_{\mathrm{e}} n_{r+1}}{n_r} = \frac{2 Z_{r+1}}{Z_r} \left(\frac{2 m_{\mathrm{e}} \pi k_{\mathrm{B}} T_{\mathrm{e}}}{h^2} \right)^{3/2} \exp\left(-\frac{E_{\mathrm{I}} - \Delta E_{\mathrm{I}}}{k_{\mathrm{B}} T_{\mathrm{e}}} \right) \tag{3}$$

Here, Equations (2) and (3) describe the dissociation and ionization processes in NLTE plasma, respectively. The reaction temperature for dissociation is selected as the heavy-particle temperature, while ionization corresponds to the electron temperature. n_i denotes the number density of species i, Z_i represents the internal partition function of species i, and m_i is the absolute mass of species i. E_{d} and E_{I} are the dissociation and ionization energies, respectively, and ΔE_{I} accounts for the reduction in ionization energy due to interparticle interactions. k_{B} and h denote the Boltzmann constant and Planck constant, respectively. Based on the multi-temperature plasma composition, the thermodynamic properties and transport coefficients of the arc can be calculated using thermodynamic equations and the Chapman-Enskog method. The detailed computational methodology has been described in our previous work [8]. Utilizing the thermophysical parameters of multi-temperature plasma, this study further conducts preliminary arc simulations and briefly compares the results with those obtained using traditional two-temperature thermophysical parameters. The behavior of the arc during interruption is described using an axisymmetric MHD model. This numerical approach treats the arc as a continuous fluid subjected to electromagnetic fields and solves the governing equations based on the Navier-Stokes equations with electromagnetic source terms. For the non-equilibrium arc model, the energy of electrons and heavy particles must be considered separately [11]:

$$\frac{\partial(\rho h_{\mathrm{e}})}{\partial t} + \nabla \cdot (\rho h_{\mathrm{e}} \vec{u}) = \nabla \cdot (k_{\mathrm{eeff}} \nabla T_{\mathrm{e}}) - Q_{\mathrm{eh}} - Q_{\mathrm{rad}} + Q_{\mathrm{J}} + \frac{5 k_{\mathrm{B}}}{2e} \vec{J} \cdot \nabla T_{\mathrm{e}} \tag{4}$$

$$\frac{\partial(\rho h_{\mathrm{h}})}{\partial t} + \nabla \cdot (\rho h_{\mathrm{h}} \vec{u}) = \nabla \cdot (k_{\mathrm{heff}} \nabla T_{\mathrm{h}}) + Q_{\mathrm{eh}} + Q_{\mathrm{rab}} \tag{5}$$

Here, u represents the mass-averaged velocity of plasma particles; ρ and h denote the density and enthalpy of the plasma, respectively, which are fundamental thermodynamic parameters of the plasma; J represents the current density at a certain point in space; k_{eff} is the effective thermal conductivity, encompassing the combined effects of laminar and turbulent flow; Q_{eh} denotes the energy exchange term between electrons and heavy particles; Q_{J} represents Joule heat; Q_{rad} represents the radiative emission energy of electrons; and Q_{rab} indicates the radiative reabsorption energy of heavy particles. For radiation calculations [12], the net emission coefficient (NEC) method was adopted in this work, with the boundary of the net emission region defined at 0.83 times the maximum temperature. Only atomic radiation was considered.

3. Multi-temperature thermophysical properties of SF_6 and C_4F_7N–CO_2

3.1. Thermodynamic properties

Figure 1 presents the thermodynamic properties of non-thermal equilibrium SF_6 plasma at 0.1 MPa. Figure 1(a) depicts the plasma density, which represents

the mass per unit volume. As temperature increases, the interparticle spacing expands, and larger molecules dissociate into smaller ones, leading to a continuous decrease in plasma density. Under non-thermal equilibrium conditions, when the electron temperature is fixed, the heavy-particle temperature decreases with increasing non-equilibrium degree, while the corresponding number density of heavy particles per unit volume rises. Consequently, as non-equilibrium conditions intensify, the plasma density increases. Additionally, lower heavy-particle temperatures suppress dissociation reactions in the system, further delaying the density decline with temperature. Moreover, in the multi-temperature model, the higher vibrational temperature of heavy species and the larger vibrational partition function of polyatomic molecules further inhibit dissociation. Thus, in the temperature range where dissociation reactions dominate, the density computed by the multi-temperature model exceeds that of the two-temperature model.

Figure 1(b) illustrates the isobaric specific heat of the plasma, reflecting the ongoing chemical reactions in the system. The peaks in the specific heat curve arise from the energy consumption of various chemical reactions. For LTE plasma, the peak around 1000∼2500 K primarily corresponds to the stepwise dissociation of SF_6 molecules. In non-thermal equilibrium plasma, dissociation reactions are suppressed due to lower heavy-species temperatures, causing the specific heat evolution to lag behind LTE conditions at lower temperatures. In high-temperature regions, according to Wu et al. [13], the electron temperature contributes θ times more than heavy particles to the non-equilibrium isobaric specific heat, leading to a significant increase in specific heat with rising non-equilibrium degree. Under multi-temperature conditions, dissociation and first-order ionization reactions are further suppressed, delaying the evolution of plasma specific heat compared to the two-temperature model. Furthermore, at lower temperatures, the higher vibrational energy of heavy species in multi-temperature plasma results in slightly greater specific heat than in the two-temperature model.

Figure 2 displays the thermodynamic properties of non-equilibrium 10% C_4F_7N–90% CO_2 plasma. Compared to SF_6, the C_4F_7N mixture exhibits more complex chemical reaction pathways, where dissociation and ionization reactions are strongly coupled and more sensitive to non-equilibrium conditions. For instance, at θ=6, the difference between multi-temperature and two-temperature models in SF_6 plasma is mainly observed below 21,000 K, whereas in the C_4F_7N mixture, the multi-temperature approach influences nearly the entire temperature range. In summary, compared to the two-temperature model, the multi-temperature model primarily affects plasma thermophysical properties by altering the vibrational energy of species and modifying chemical reaction dynamics, with the latter having a more pronounced impact.

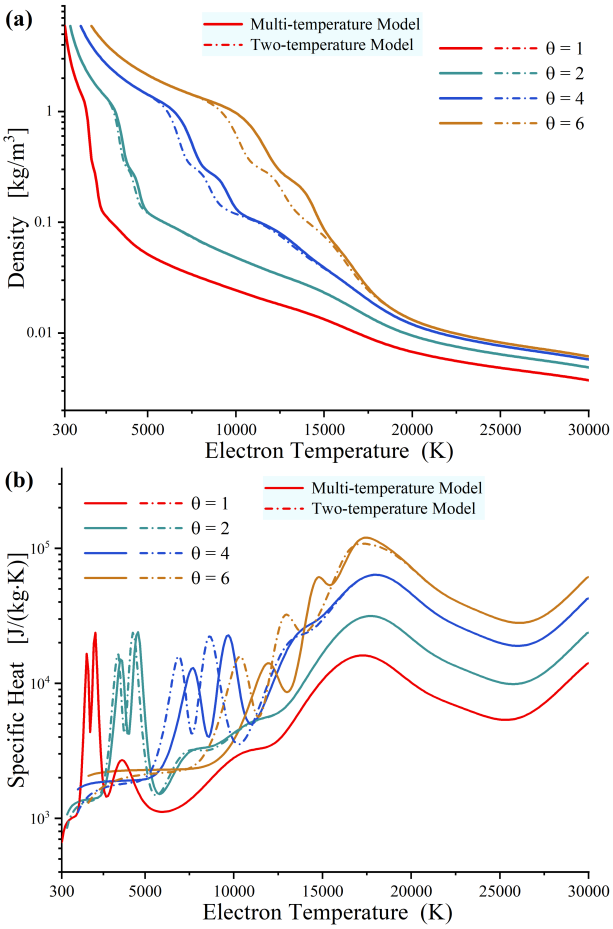

Figure 1. Thermodynamic properties of non–equilibrium SF_6 at 0.1 MPa.

3.2. Transport coefficients

Figure 3 presents the transport coefficients of SF_6 at 0.1 MPa under non-equilibrium conditions. Figure 3(a) shows the electrical conductivity, which primarily characterizes electron transport in the plasma. In the low-temperature regime, the reduced heavy-particle temperature in NLTE plasma suppresses dissociation and ionization reactions, leading to lower electron number density and consequently decreased electrical conductivity. In contrast, at high temperatures where ionization reactions dominate, the higher heavy-particle number density in non-equilibrium plasma results in relatively greater electron number density, causing conductivity to increase with non-equilibrium degree. Compared to the two-temperature model, multi-temperature plasma exhibits lower conductivity in the low-temperature region but remains consistent at high temperatures. This occurs because the multi-temperature definition primarily influences chemical reaction progress without directly altering the total particle number density per unit volume.

Figure 3(b) depicts viscosity, which mainly reflects heavy-particle transport processes. As non-equilibrium degree increases, the reduced heavy-species temperature weakens interparticle interactions, thereby decreasing viscosity. Furthermore, since non-

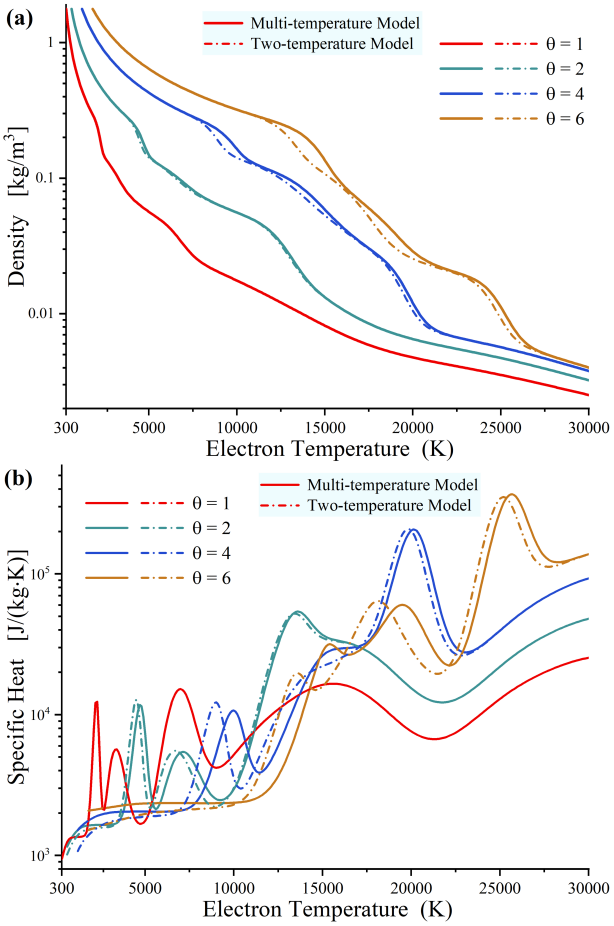

Figure 2. Thermodynamic properties of non–equilibrium C_4F_7N mixture at 0.1 MPa.

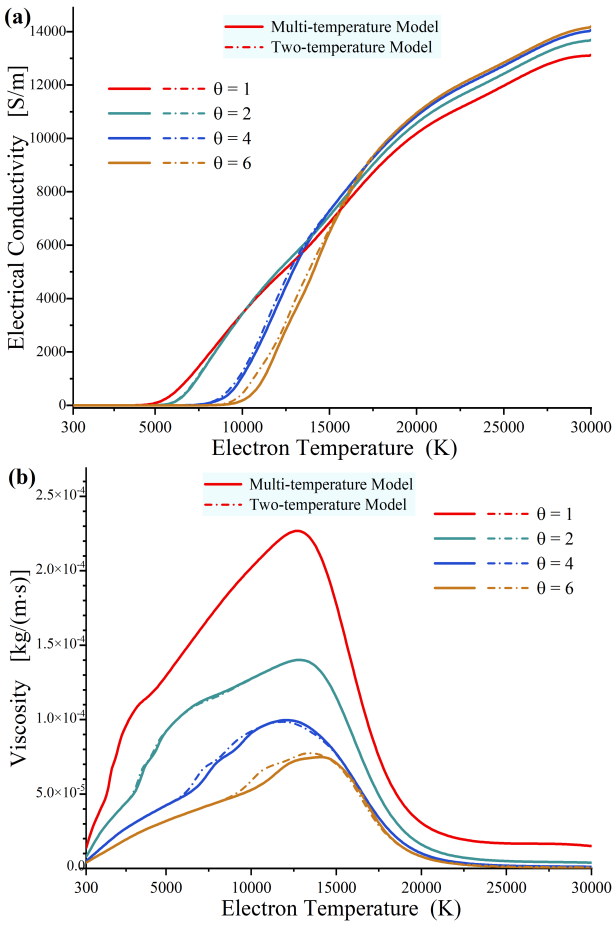

Figure 3. Transport coefficients of non-equilibrium SF_6 at 0.1 MPa.

equilibrium conditions inhibit dissociation reactions in the plasma, the viscosity peak under NLTE conditions shifts toward higher electron temperatures. Compared to the two-temperature model, multi-temperature plasma exhibits slower viscosity evolution, collectively demonstrating a "stronger non-equilibrium state."

Figure 4 displays the transport coefficients of 10% C_4F_7N–90% CO_2 plasma under non-thermal equilibrium. Similar to thermophysical properties, the multi-temperature model exerts more pronounced effects on transport coefficients in C_4F_7N mixtures than in SF_6. For instance, at θ=6, the difference between multi-temperature and two-temperature models in SF_6 plasma is primarily confined below 18,000 K, whereas for C_4F_7N mixtures, this influence persists up to 26,000 K. This demonstrates that the multi-temperature definition predominantly affects plasma transport coefficients by modifying chemical reaction progress. Given the more intricate chemical reaction pathways in C_4F_7N-based mixtures, multi-temperature conditions exhibit a more pronounced influence on the thermophysical properties of C_4F_7N arc plasmas.

4. MHD simulation of multi-temperature arcs

This study is based on a simplified switching arc model: during the reverse motion of the contacts, the arc burns within a classical converging-diverging nozzle while a constant gas blow is applied on one side. The current is maintained at a constant 50 A, and when the electrode reaches a certain reverse displacement, the current is rapidly reduced to 0 A to simulate the arc extinction process. The background pressure during arc burning is 0.1 MPa.

Figure 5 presents the temperature and non-equilibrium degree distributions of a 10% C_4F_7N–90% CO_2 arc under both multi-temperature and two-temperature models, captured at a steady current of 50 A during sustained arc burning. During arc combustion, two distinct non-equilibrium layers emerge at the arc periphery–one in the high-temperature region immediately adjacent to the arc edge and another in the lower-temperature region farther outward. For the inner non-equilibrium layer near the arc edge, the electron temperature ranges between 7,000∼8,000 K, primarily due to the steep temperature gradient and frequent gas flow exchange in this region, which hinder the complete and rapid transfer of Joule heating from electrons to heavy particles. The non-equilibrium de-

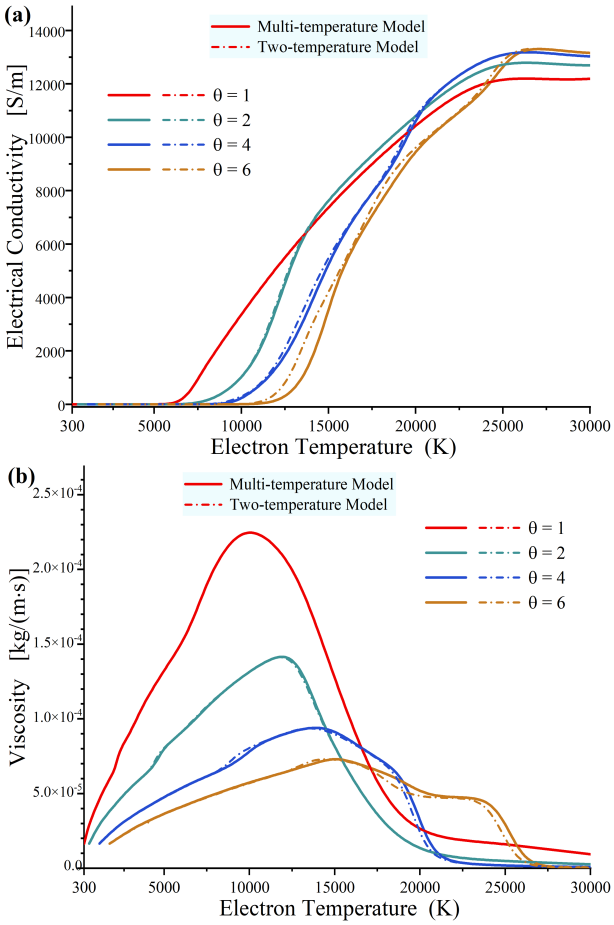

Figure 4. Transport coefficients of non-equilibrium C_4F_7N mixture at 0.1 MPa.

gree in this layer is approximately 1.5. In contrast, the outer non-equilibrium layer exhibits electron temperatures below 4,000 K, where insufficient energy exchange between electrons and heavy particles results in a pronounced non-equilibrium state, with a non-equilibrium degree reaching up to 3.5 (indicating strong NLTE conditions).

Furthermore, compared to the conventional two-temperature model, the mlti-temperature arc exhibits a more significant non-thermal equilibrium effect. In the high-temperature inner non-equilibrium layer, the multi-temperature model yields a non-equilibrium degree of 1.5, whereas the two-temperature model predicts 1.3. At the cooler outer arc boundary, the multi-temperature model produces a thicker outer non-equilibrium layer than the two-temperature model. This discrepancy arises because, in the two-temperature model, electron collision energy directly increases heavy-particle temperature, whereas in the multi-temperature model, a portion of this energy is additionally allocated to elevating vibrational temperature. Moreover, suppressed ionization reactions in multi-temperature plasma lead to slightly lower electron density compared to the two-temperature model, further reducing electron-heavy particle energy transfer efficiency.

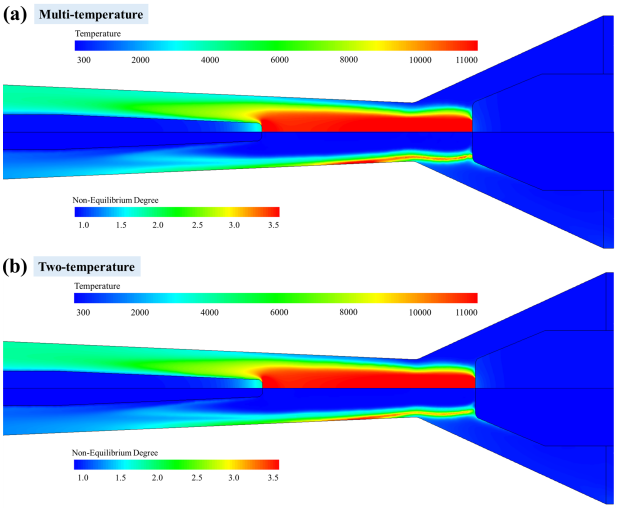

Figure 5. MHD simulation results of non-thermal equilibrium C_4F_7N mixture arc: (a) Multi-temperature model, (b) Two-temperature model.

For the arc extinction process, the influence of the multi-temperature model on MHD simulation results is similar to that during the arcing period. Under different temperature definitions, the temperature and non-equilibrium degree distributions exhibit nearly identical characteristics. The only distinction is that the multi-temperature model yields slightly higher calculated values for plasma non-equilibrium degree. This finding suggests that for most computational scenarios, the simpler two-temperature model can adequately meet accuracy requirements. The rationale lies in the fact that when the non-equilibrium degree is low, the thermophysical properties of arc plasma show minimal differences between the two-temperature and multi-temperature approaches. However, in practical high-voltage circuit breakers, the plasma's non-equilibrium degree may become significantly larger due to intense gas blowing and turbulent effects. Under such conditions, the impact of multi-temperature definitions may need to be re-evaluated to ensure simulation fidelity.

5. Conclusions

At the arc periphery and current-zero regions, arc plasmas typically exist in a non-thermal equilibrium state. This study investigates the thermodynamic properties of NLTE SF_6 and C_4F_7N–CO_2 plasmas and conducts MHD simulations of NLTE arc plasmas based on a simplified arc model.

Non-equilibrium conditions significantly influence the thermophysical properties and transport coefficients of plasmas, primarily due to substantial alterations in chemical reaction pathways and species composition within NLTE plasmas, as well as changes in total particle number density. Compared to the conventional two-temperature model, the multi-temperature definition induces notable variations in plasma thermophysical parameters, particularly un-

der strong non-equilibrium conditions. Owing to the molecular complexity of C_4F_7N mixtures, their thermophysical properties exhibit more pronounced sensitivity to non-equilibrium conditions and multi-temperature definitions than those of SF_6. Furthermore, the conventional two-temperature model may slightly underestimate the non-equilibrium degree. Under the simplified arcing conditions examined in this work, the multi-temperature model demonstrates lesser influence, suggesting that the two-temperature model remains a simpler and acceptable approach. However, in practical circuit breaker environments characterized by intense ablation and strong gas blowing effects, plasma non-equilibrium phenomena may become significantly more pronounced. In such cases, the impact of multi-temperature states states may require more thorough consideration.

Acknowledgements

The work was supported by the National Natural Science Foundation of China (52422707, 524B2105).

References

[1] A. B. Murphy and E. Tam. Thermodynamic properties and transport coefficients of arc lamp plasmas: argon, krypton and xenon. *J. Phys. D Appl. Phys.*, 47(29):295202, 2014. doi:10.1088/0022-3727/47/29/295202.

[2] V. R. T. Narayanan, M. Gnybida, and C. Rümpler. Transport and radiation properties of C_4F_7N-CO_2 gas mixtures with added oxygen. *J. Phys. D Appl. Phys.*, 55(29):295502, 2022. doi:10.1088/1361-6463/ac6af5.

[3] J. Annaloro, P. Teulet, A. Bultel, et al. Non-uniqueness of the multi-temperature law of mass action. Application to 2T plasma composition calculation by means of a collisional-radiative model. *Eur. Phys. J. D*, 71(342):1–14, 2017. doi:10.1140/epjd/e2017-80284-5.

[4] V. Colombo, E. Ghedini, and P. Sanibondi. Two-temperature thermodynamic and transport properties of carbon–oxygen plasmas. *Plasma Sources Sci. T.*, 20(3):035003, 2011. doi:10.1088/0963-0252/20/3/035003.

[5] W. Wang, J. D. Yan, M. Rong, et al. Theoretical investigation of the decay of an SF_6 gas-blast arc using a two-temperature hydrodynamic model. *J. Phys. D Appl. Phys.*, 46(6):065203, 2013. doi:10.1088/0022-3727/46/6/065203.

[6] X. Li, H. Zhao, and A. B. Murphy. SF_6-alternative gases for application in gas-insulated switchgear. *J. Phys. D Appl. Phys.*, 51(15):153001, 2018. doi:10.1088/1361-6463/aab314.

[7] P. Pietrzak, J. T. Engelbrecht, D. Kumari, and C. M. Franck. Short-line fault interruption performance comparison of SF_6 alternatives. *IEEE Trans. Power Delivery*, 39(6):3071–3081, 2024. doi:10.1109/TPWRD.2024.3451178.

[8] G. Wang, B. Zhang, M. Cao, et al. Two-temperature thermodynamic and transport properties of C_4F_7N-CO_2-O_2 mixture as an arc-extinguishing gas. *J. Phys. D Appl. Phys.*, 58(16):165502, 2025. doi:10.1088/1361-6463/adbcbd.

[9] X. Baumann, P. Teulet, Y. Cressault, and A. Bultel. Study on reaction rates for 2T SF_6 plasma: application to chemical kinetics of a decaying arc in high voltage circuit breakers. *J. Phys. Conf. Ser.*, 1243:012007, 2019. doi:10.1088/1742-6596/1243/1/012007.

[10] P. André, M. Abbaoui, A. Augeard, et al. Study of condensed phases, of vaporization temperatures of aluminum oxide and aluminum, of sublimation temperature of aluminum nitride and composition in an air aluminum plasma. *Plasma Chem. Plasma Process*, 36:1161–1175, 2016. doi:10.1007/s11090-016-9704-7.

[11] Y. Cressault, P. Teulet, X. Baumann, and A. Gleizes. Non-equilibrium phenomena in thermal plasmas. *Plasma Res. Express*, 2(4):043001, 2020. doi:10.1088/2516-1067/abc1b9.

[12] X. Baumann, P. Teulet, Y. Cressault, and A. Bultel. Radiative properties and numerical modeling of C_4F_7N-CO_2 thermal plasma. *Plasma Phys. Technol.*, 6(2):144–147, 2019. doi:10.14311/ppt.2019.2.144.

[13] W. Wang, M. Rong, Y. Wu, et al. Two-temperature thermodynamic and transport properties of SF_6–Cu plasmas. *Phys. Plasmas*, 19(8):083506, 2012. doi:10.1063/1.4739778.